Journal of Electronics and Electrical Engineering
https://ojs.wiserpub.com/index.php/JEEE

Research Article

Modeling and Simulation of Microgrid Dynamic Operation Modes Using MATLAB Simulink Software

Vu Hoa Nguyen, Tien Dat Tran, Minh Khoa Ngo*

Faculty of Engineering and Technology, Quy Nhon University, Quy Nhon, Vietnam
*Correspondence: ngominhkhoa@qnu.edu.vn

Received: 16 September 2024; **Revised:** 9 November 2024; **Accepted:** 12 November 2024; **Published:** 15 November 2026

Abstract: Microgrids are one of the effective solutions for utilizing renewable energy sources and distributed generations in distribution networks. This paper proposes a model to study operation modes of a microgrid consisting of a battery energy storage system (BESS), a solar power system, a diesel generator, a main grid and consumers. The microgrid components and control systems are modelled in the MATLAB Simulink software. Based on this model, different operating scenarios including the islanded mode and the black start mode are carried out to analyse and evaluate the dynamic response of the microgrid. The voltage, current, power, and frequency at various locations in the system are simulated under these scenarios. The results indicate that, with the support of BESS control, the microgrid maintains stable operation in both studied modes.

Keywords: battery energy storage system, black start, distribution network, islanded mode, solar power system

1. Introduction

Many scientists are focusing on finding solutions to improve the efficiency of renewable energy integration into the existing grid. These solutions are recognized as one of the important criteria to improve power supply reliability, reduce energy loss, and operate flexibly power systems [1–3]. The microgrid is considered as a technique to enhance the renewable energy integration and optimization participating in the grid, such as wind power plants, solar power plants, diesel generators, Battery Energy Storage Systems (BESS) [4, 5]. The integration of microgrids into electrical systems is garnering significant interest due to their numerous advantages. These include facilitating more sustainable operations by incorporating local renewable energy sources such as wind and solar; lowering energy costs through optimized demand management, energy storage solutions, and the resale of electricity to the grid during peak demand periods; and improving reliability to ensure continuous power supply to facilities during outages [6]. Furthermore, this model can be utilized to deliver electricity to remote regions that are not connected to the main power grid.

Compared to traditional power systems, islanded microgrids have a low system inertia. Additionally, distributed generations using renewable energy sources have fluctuating, random, and interrupted output power, making it difficult to control and balance power in the power system [7]. The challenge for islanded microgrids is to ensure that the power balance between generations and loads is always balanced when there is a power change to stabilize the frequency and voltage, as well as having high compatibility, so it is necessary to have a source that is able to regulate and respond quickly

DOI: https://doi.org/10.37256/jeee.3220245693

[8]. Microgrids also play an important role with customer participation in power generation, energy storage, control, and management in the grid. This development converts consumers into professional consumers and allows them to take an active role in the grid [9, 10]. The integration of microgrids into the existing distribution system has transformed it from a passive grid into an active grid [11, 12].

Recently, researchers have focused on exploring various aspects of microgrids, including studies on efficient energy management systems for small-scale hybrid solar microgrids [13], optimizing the operation of microgrids using renewable energy sources, investigating distributed economic operation in smart grids [14] and addressing challenges related to microgrid protection and methods for mitigating the impacts of these challenges [15–17]. Additionally, modeling and simulating the operational modes of a microgrid for research purposes is a significant topic of interest, such as dynamic simulations of microgrid systems for universities and simulations of the coordination between Battery Energy Storage Systems (BESS) and photovoltaic (PV) systems with bidirectional power control strategies in microgrids [18–20]. The simulation results from various scenarios contribute to the design calculations and rational operation of microgrids. Consequently, this paper focuses on the modeling and simulation of a microgrid using MATLAB/Simulink software. This microgrid includes essential components such as a Battery Energy Storage System (BESS), a photovoltaic (PV) system, a diesel generator, grid power, and electrical loads. The integration of the BESS enhances the stability of the microgrid studied in this model. The microgrid is analyzed under two operational modes: islanding mode and black start mode. The novel contributions of this paper include: (i) Establishing a microgrid model with components such as the photovoltaic system, BESS, and diesel generator; (ii) Analyzing and evaluating the operational capability of the microgrid while operating in islanding mode; (iii) Verify the operation ability of the black start mode and study the microgrid dynamic responses under the disturbances.

2. Proposed microgrid test system model

A microgrid consists of distributed energy sources, microturbine sources (diesel generators, thermal power plants, and small hydro power plants), battery energy storage systems, consumers, and these elements can be managed through a central control system as depicted in Figure 1. Based on the central control system, the microgrid can operate in grid-connected, island-separated modes or can flexibly switch between these two modes as needed [21]. In the microgrid, the microturbine and BESS play a key role in controlling power, voltage, and frequency stability. The BESS responds quickly to disturbances in renewable energy sources to regulate the power system frequency and voltage [22]. Besides, the storage capacity is also a very important factor, it means the proportion of energy available after a full charge and upon self-discharge and the proportion of time required to reach the deep discharge capacity [23].

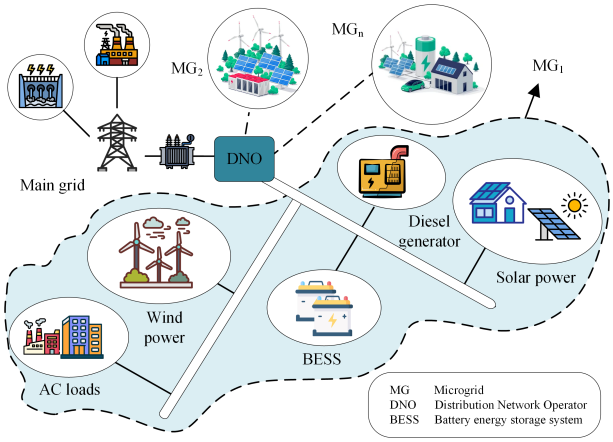

Figure 1. Microgrid overview

2.1 *System configuration*

The microgrid model proposed for studying in this paper is depicted in Figure 2 that consists of main components: a BESS, a solar power system, a diesel generator, a main grid, consumers and a central control system [24, 25]. In particular, the diesel generator, which plays a backup source in the microgrid, is equipped with frequency and excitation control systems to control its generation power and voltage. On the other hand, the solar power system and the BESS are main sources to supply energy for the microgrid. The solar power system is connected via an inverter. The BESS has also the controllers to receive commands and setpoints from the central control system, operating with many modes, such as the grid-following, grid-forming, or resynchronization [26].

During normal operation, the microgrid remains connected to the main grid. In case of disturbances, however, the microgrid disconnects and switches to islanded mode. In islanded mode, a section of the distributed network becomes electrically isolated from the main grid, and loads are supported solely by local distributed generation sources. These distributed sources are typically power-electronic-based, adding complexity to the study of the system as a whole [27].

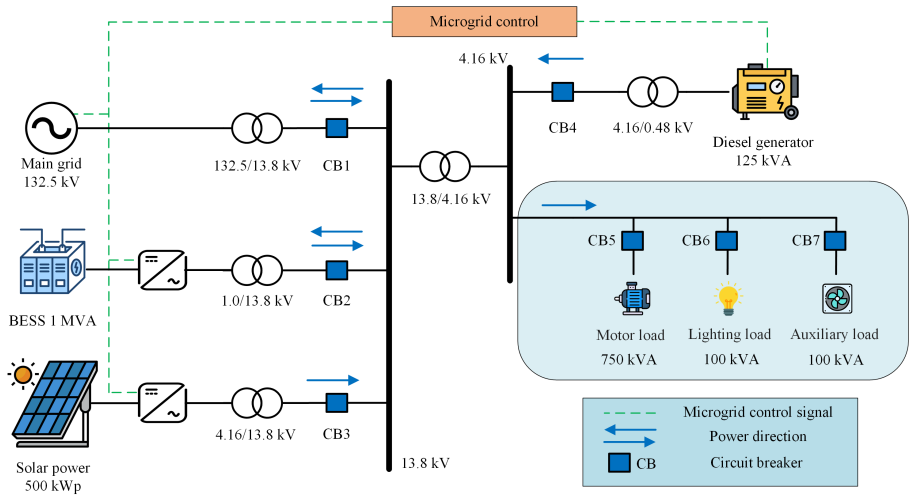

Figure 2. Proposed microgrid test system model

In this system configuration, the solar power system consists of two parallel chains with 100 panels in series and total peak power of 500 kWp. The solar power system is assumed to operate at the irradiance of 1,000 W/m^2 and the temperature of 25 °C. The diesel generator has the capacity of 125 kVA, the rated voltage of 480 V, and the rated frequency of 50 Hz. The step-up transformer is used to increase the output voltage for the diesel generator from 0.48 kV to 4.16 kV for supplying the loads. The main grid has the rated voltage of 132.5 kV, the rated frequency of 50 Hz, and the total power impedance of 2 Ω. Furthermore, the system includes three major categories of loads, such as the 100-kVA lighting load, the 100-kVA auxiliary load, and the 750-kVA motor load. The BESS will respond rapidly to variations in the microgrid. It includes main components, such as battery modules, grid-side converters, filters, transformers, measurement, and control systems. This BESS has a total power capacity of 1 MVA and a DC output voltage of 2.2 kV. The converter creates an AC voltage of 1 kV from a DC output voltage of 2.2 kV and connects it to the system via a 1-MVA transformer with a primary voltage of 1 kV and a secondary voltage of 13.8 kV.

2.2 *Main components*

Figure 3 illustrates the mask creation blocks for the BESS, while Figure 4 shows the control blocks within MATLAB Simulink. These control blocks are designed to manage the BESS during power fluctuations, allowing the microgrid to seamlessly switch between different operating modes, such as grid-following, grid-forming, and resynchronization.

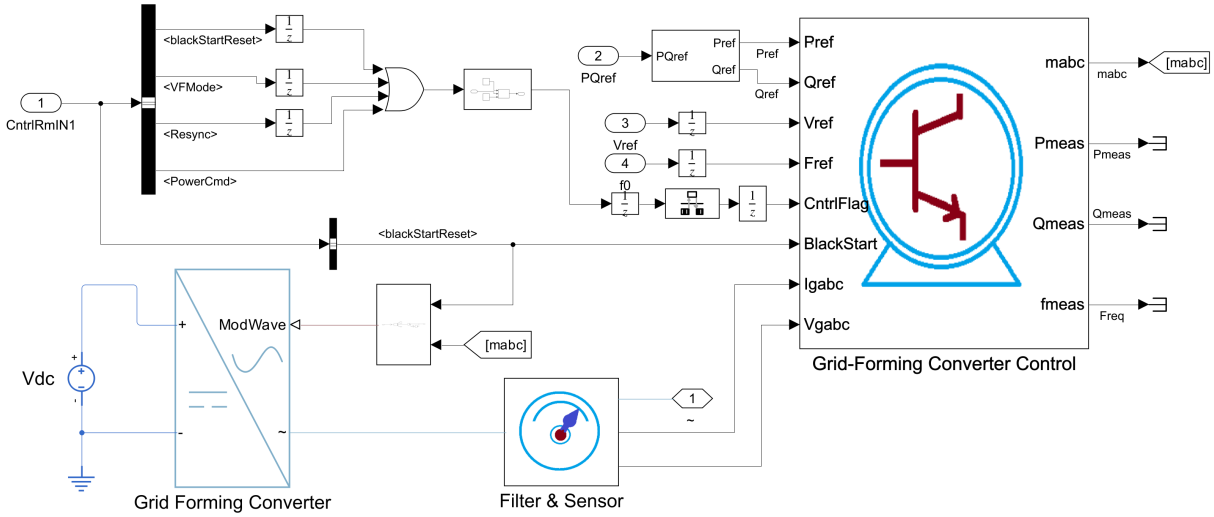

Figure 3. BESS modeling blocks in MATLAB Simulink

According to Figure 4, the main components of the BESS control system are the measurement unit, the power control unit, the voltage and current control unit. The measurement unit is used to compute the frequency and active and reactive power generated by the inverter. It also computes the *d-q* components of the three-phase voltage and current at the microgrid point of common coupling (PCC) bus. In the grid-following mode, the power control unit is active to regulate the active and reactive power by using the measured power at the BESS primary bus and the power reference signals *Pref* and *Qref* to generate the *activeControl*, *reactiveControl*, and *angle* signals. In grid-forming mode, the voltage control unit is active to regulate the three-phase voltages at the PCC bus. For the current control, the regulators process the measured and reference currents to produce the required d-q voltages for the inverter.

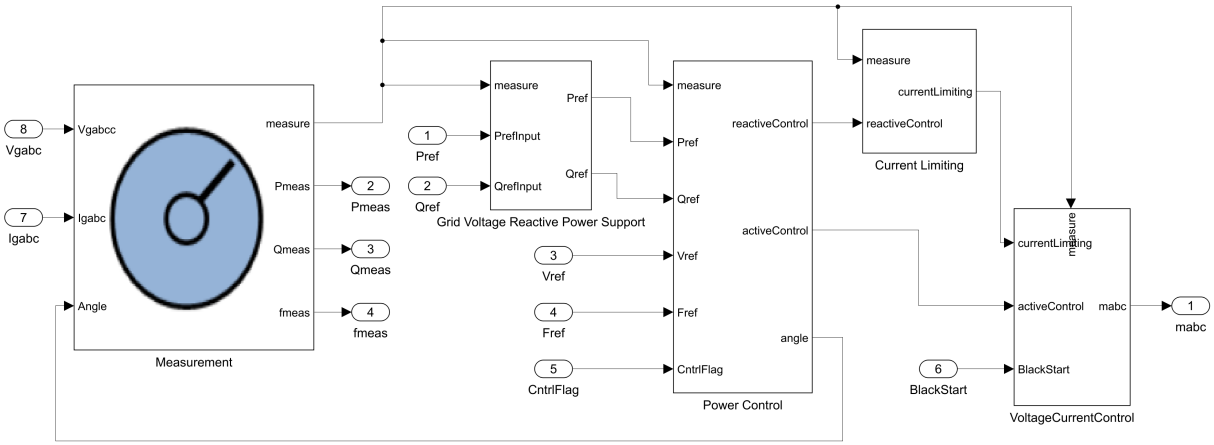

Figure 4. BESS control system in MATLAB simulink

The BESS power at the time t ($P_{\mathrm{BESS},t}$) can be positive or negative. If $P_{\mathrm{BESS},t} > 0$ the BESS is discharging and acting as a generator, unless $P_{\mathrm{BESS},t} < 0$ the BESS is charging and acting as a load. The value of $P_{\mathrm{BESS},t}$ is constrained by the following equation:

$$P_{\text{BESS}}^{\min} \leq P_{\text{BESS},t} \leq P_{\text{BESS}}^{\max} \tag{1}$$

Besides, SoC_t is the state-of-charge of the BESS at the time t. SoC_t is within the range between the minimum and maximum of the state-of-charge to ensure the battery life span.

$$SoC^{\min} \leq SoC_t \leq SoC^{\max} \tag{2}$$

where $SoC^{\min}$ and $SoC^{\max}$ are the minimum and maximum of the state-of-charge of the BESS, respectively.

The diesel generator is another essential component that helps stabilize system parameters such as frequency and voltage, and it can supply power to the system in all operational scenarios as required by the controller. Figure 5 shows the diesel generator model in MATLAB Simulink. In conjunction with Figure 1, the diesel generator is connected to a 4.16 kV busbar to efficiently supply power to the load while also stabilizing the grid when the Battery Energy Storage System (BESS) is in a charging state.

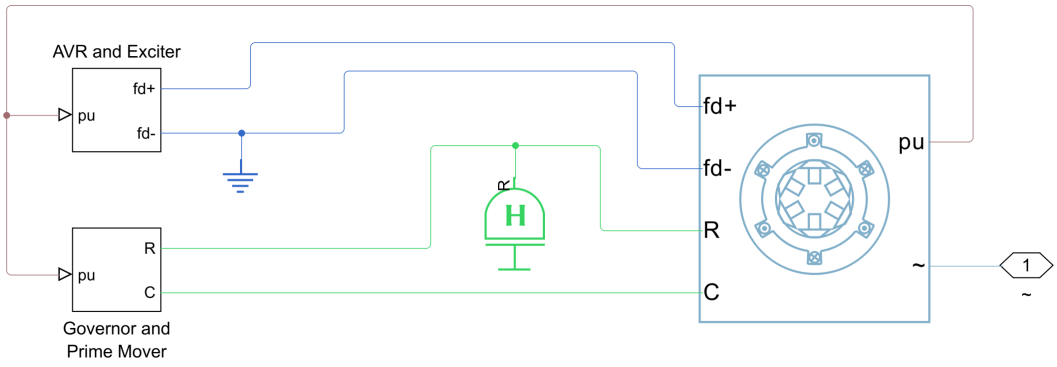

Figure 5. Diesel generator model in MATLAB simulink

The renewable energy source used in the model is a solar power system. It supplies power to the system, reducing reliance on the main power grid and thereby optimizing costs. After conversion by the inverter, the solar power system is fed through a transformer to a 13.8 kV busbar to provide power and support transmission. The solar power system model is illustrated in Figure 6, which includes the photovoltaic (PV) panel array and inverter systems.

The output power of this solar power system is calculated as follows:

$$P_{PV} = f_{PV} P_{PV,R} \left(\frac{G_T}{G_{T,STC}} \right) \left[1 + \alpha_P \left(T_{cell} - T_{cell,STC} \right) \right] \tag{3}$$

where P_{PV} is the output power of the PV system (kW); f_{PV} is the derating factor, reflecting the impact of dust on the surface, lifespan, and other factors on the output power; $P_{PV,R}$ is the rated power of the PV system (kW); G_T is the actual solar radiation (kW/m^2); $G_{T,STC}$ is the solar irradiance under Standard Test Conditions (STC) (kW/m^2); α_P is the temperature coefficient of the power source; T_{cell} is the temperature of the PV cell (°C); $T_{cell,STC}$ is the temperature of the PV cell under standard test conditions with T value of 25 (°C).

In this model, the load system consists of lighting loads, auxiliary loads, and motor loads. All loads can be controlled through Circuit Bbreakers (CB) positioned in front of them. Additionally, the motor load includes a dedicated controller to regulate load power, enabling black start operations and flexible load power adjustments within the system. Figure 7 shows the load model in MATLAB Simulink, including the components mentioned above as well as those in Figure 2.

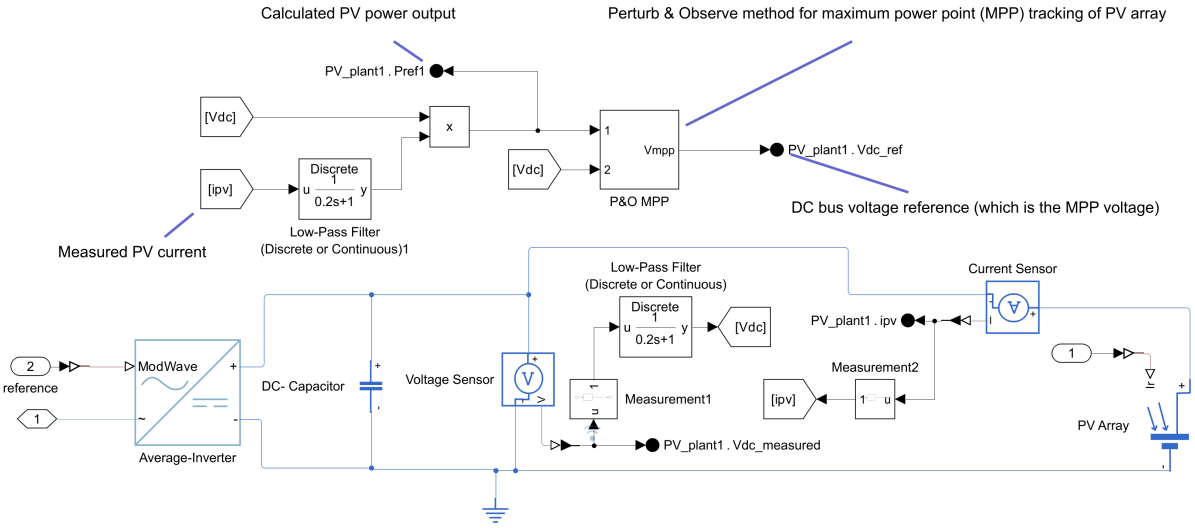

Figure 6. Solar power model in MATLAB simulink

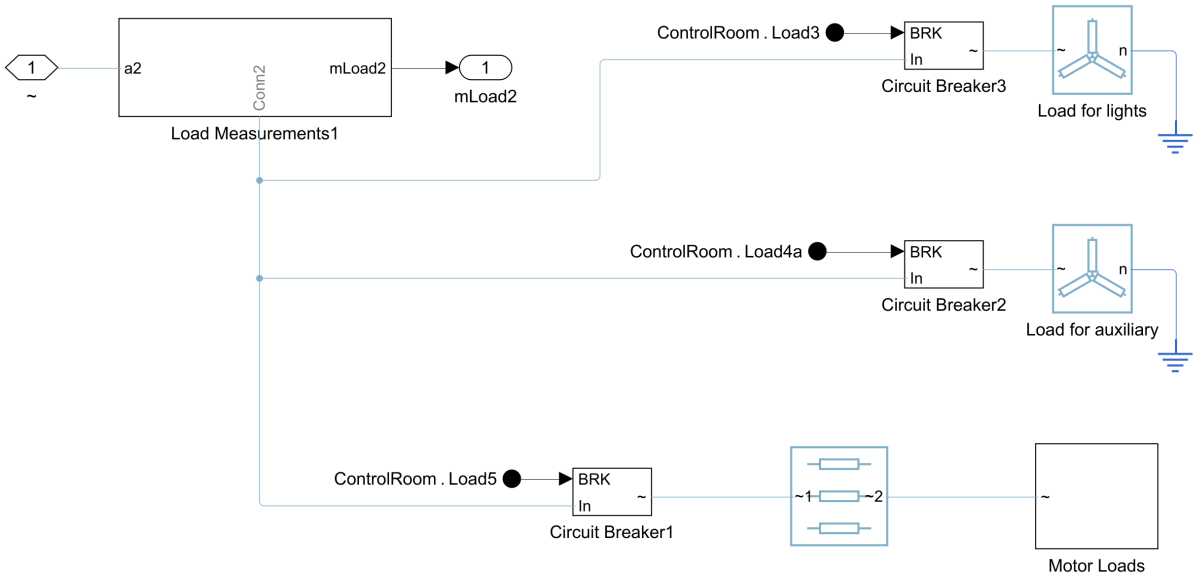

Figure 7. Load model in MATLAB simulink

To ensure that the components operate, interconnect, and function stably while facilitating flexible transitions between modes, a controller has been integrated into the model to manage the overall operation of the microgrid. This model is illustrated in Figure 8.

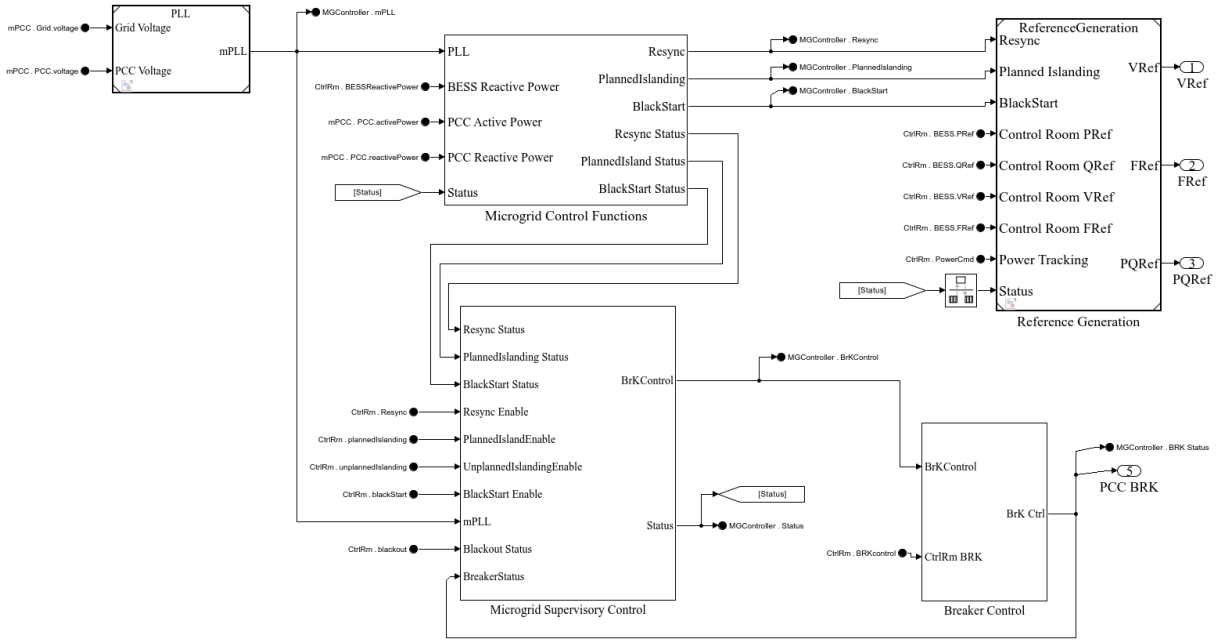

Figure 8. Microgrid controller model in MATLAB simulink

3. Numerical simulation results and discussion

From the above studied modeling, this paper focuses on simulating two typical operation modes, including the islanded mode and black start mode.

3.1 *The islanded mode*

In the islanded operation mode, the microgrid will be disconnected from the main grid at the PCC bus following a grid outage or as scheduled, and that the distributed generations, battery energy storage systems, and loads within the microgrid will be independently operated [28]. In this scenario, the microgrid test system will be simulated during a power outage of the main grid, therefore, the microgrid will be operated in the islanded mode. At this time, the BESS will be controlled to stabilize the power, voltage and frequency of the microgrid. The loading power will be supplied by the solar power system, the diesel generator, and the BESS. Figure 9 shows the frequency, voltage angle and peak voltage variations of the main grid and microgrid in islanded mode. In this figure, the simulation results are zoomed at the islanding command time of 7.96 s.

Figure 10 shows the three-phase voltage waveforms, the output current waveforms of the BESS and the main grid. When there is a islanding command, the main grid current gradually drops to zero. After appropriately 4 s, the circuit breaker and the microgrid island separation process are completed at the time of 7.96 s, the voltage and current of the BESS gradually stabilize within the acceptable limits, indicating that the test system has successfully changed to the stable islanding operation mode. If the BESS voltage and current are unstable or fall outside the permissible range, the control system must be inspected and adjusted. It can be observed that before the test system is operated under its islanded mode, the BESS current was relatively large, showing that at this time the BESS is generating the power for the loads and the main grid is only a supplementary source. After the main grid is disconnected, the microgrid is change to the islanded mode and the main grid current will drop to zero, and the BESS current also decreases due to the solar power system penetration.

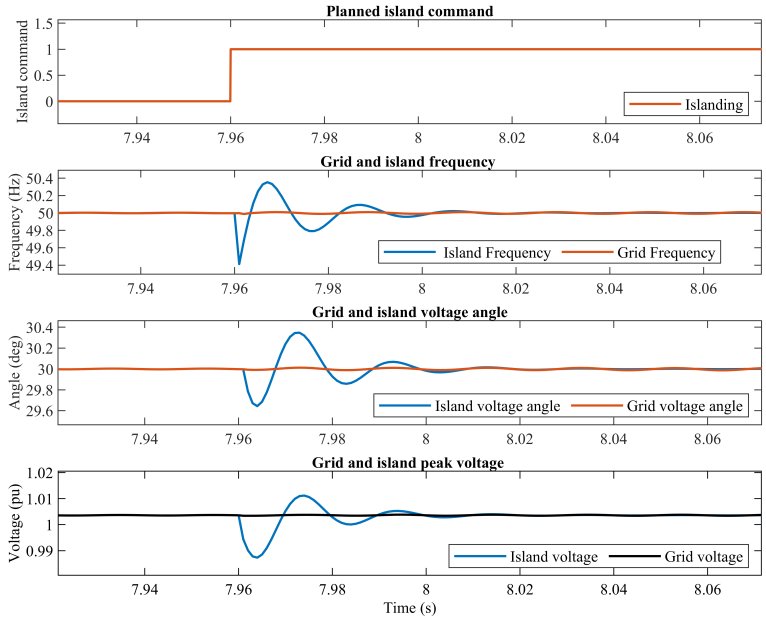

Figure 9. Frequency, voltage angle and peak voltage of main grid and microgrid in islanded mode

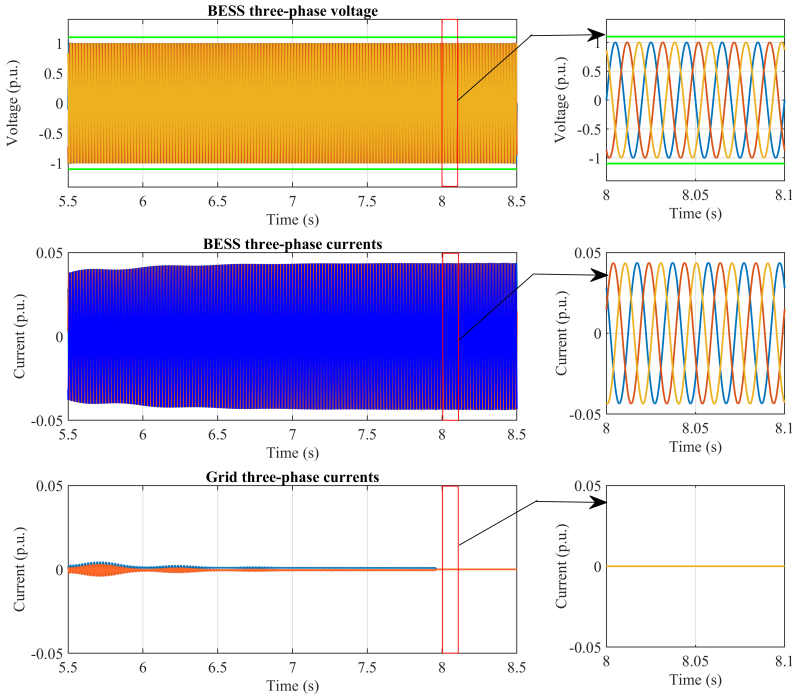

Figure 10. Three-phase voltage and current of BESS and main grid in islanded mode

Figure 11 shows the load three-phase voltage and current of the microgrid test system in the islanded operation mode. It can be obviously seen that the voltage and current tend to decrease before the time of 4 s due to the load variations, and after the reverse separation from the time of 7.96 s, the load current stabilizes and shows small variations. This indicates that the load voltage and current are still remained in a stable condition during the islanding process, demonstrating effective control and stability.

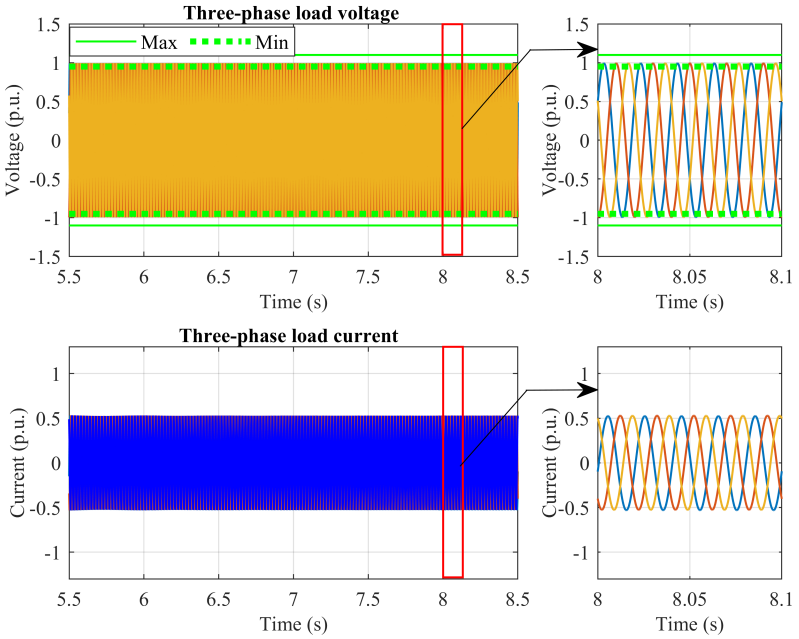

Figure 11. Load three-phase voltage and current in islanded mode

The active and reactive power of the BESS are illustrated in Figure 12. As shown in this figure, the load power is slightly over 0.5 MW, while the main grid power drops to 0 MW. At the time of 7.96 s, the BESS power is negative because the solar power system and the diesel generator are generating active power to the microgrid. Thus, the islanding process finishes, the load power is supplied by the PV system and the diesel generator. The BESS is changed to the frequency and voltage control mode to respond to the disturbance in the microgrid. After the time of 7.96 s, the BESS is charging because it is absorbing the excess power generated by the solar power system. Since the microgrid is operated in the islanded mode and cannot generate the active power to the main grid, the BESS absorbs power to recharge and maintain reserves for future operations.

3.2 *The black start mode*

The black start mode is the generation ability to restart parts of the distribution network to recover from a blackout of the main grid. This requires isolated power stations being started individually and gradually reconnected to one another to form an interconnected system again. It is used when the main grid experiences a blackout and must be restarted from scratch. As such, the black start is a critical resource for maintaining the reliability and resilience of the distribution network and is central to system restoration and recovery plans for power system operators [29]. The purpose of this work is to check the operating status of the BESS as well as whether the microgrid meets the requirements when the microgrid is operated in reverse separation mode. In this case, the black start mode is carried out at the time of 3 s, the BESS discharges enery to the microgrid and the black start process begins at the time of 4 s. The BESS output voltage increases in step by

step as defined by the black start parameters. The voltage steps and the delay between each step can be specified in the input data program file.

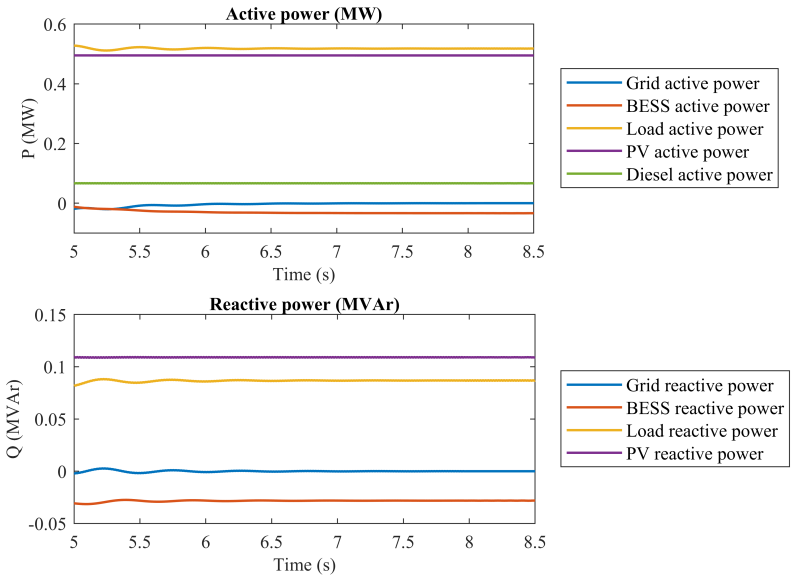

Figure 12. Active and reactive power of BESS, main grid, solar power system, and loads in islanded mode

Figure 13 illustrates the three-phase voltage and current of the BESS, as well as the current from the main grid during the black start process. In this mode, it is clearly observed that the BESS three-phase voltage and current change incrementally, demonstrating the BESS's response capability and the microgrid's operation. Starting from 7.3 s, the BESS three-phase voltage and current stabilize, indicating the successful initiation of black start mode and that the microgrid is now supplying power to the loads. Additionally, the final plot in Figure 12 shows that the main grid current is zero, as the microgrid is operating in islanded mode.

Figure 14 shows the three-phase voltage and current of the loads. When the black start process begins, the BESS de-charges for supplying an energy to the loads of the microgrid. Thus, the load voltage starts at a much lower value, below the minimum steady state one. As the black start process is started, the load power increases gradually according to the various levels. Figure 15 shows that the load three-phase voltage and current become stable, indicating that the black start control process is stable. Figure 15 illustrates the active and reactive power of the Battery Energy Storage System (BESS), the solar system, the main grid, and the electrical loads. During this process, the BESS provides both active and reactive power to the microgrid in black start mode, while the solar energy system and diesel generator are not operational in this mode. According to this graph, the system begins to restore the load from a state of collapse at the time of 5.5 s. Besides, the load is reintroduced incrementally to avoid overloading the system, ensuring it can respond effectively. By 7.3 s, the system has successfully restored the entire load, with the BESS continuing to supply stable active and reactive power to the loads. This demonstrates both reliable power provision and effective system control.

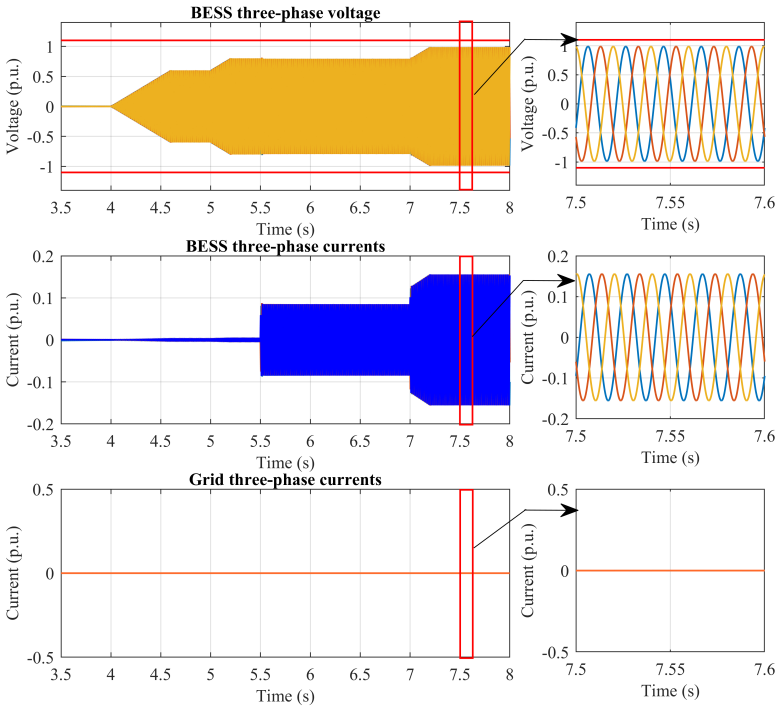

Figure 13. Three-phase voltage and current of BESS and main grid in black start mode

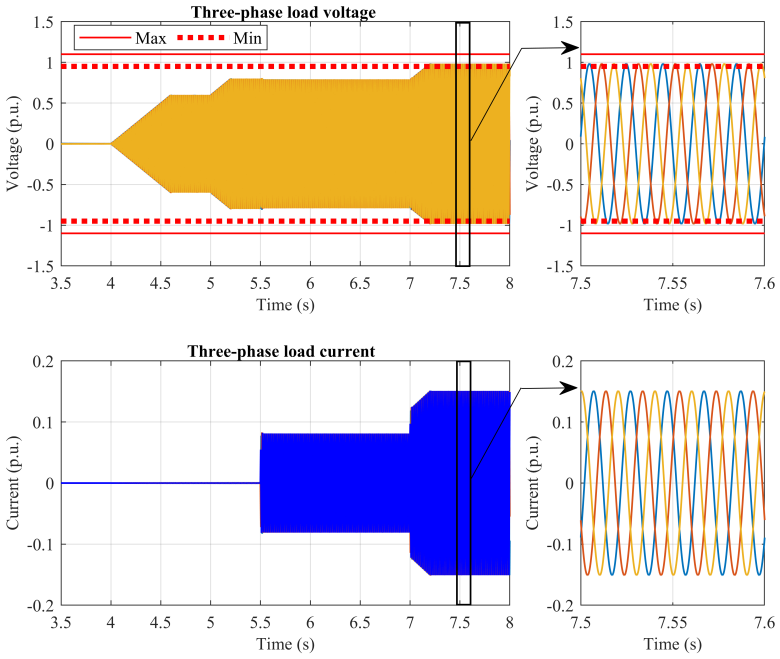

Figure 14. Load three-phase voltage and current in black start mode

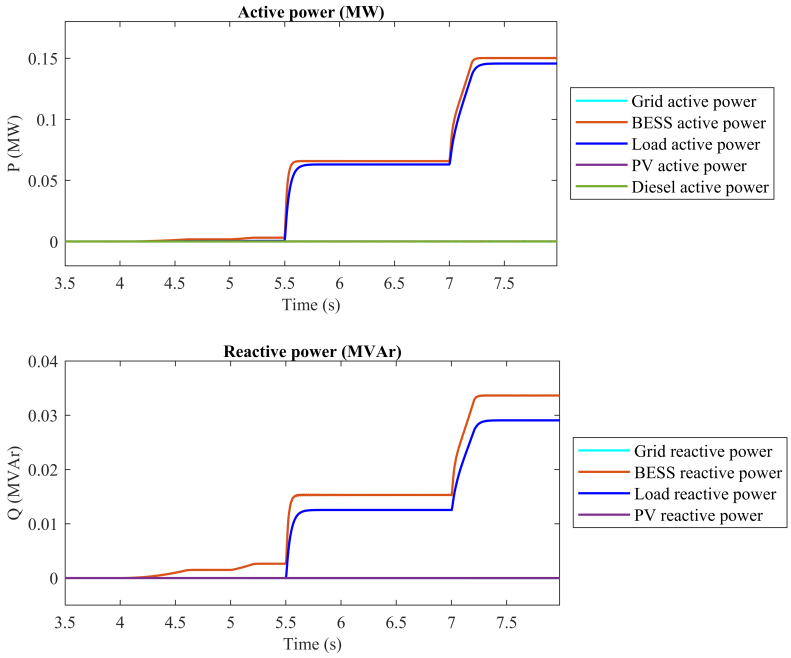

Figure 15. Active and reactive power of BESS, main grid, solar power system, and loads in black start mode

4. Conclusions

The paper studied modeling and simulation of the operation modes of a microgrid including the Battery Energy Storage System (BESS), the diesel generator, the solar power system, the main grid, and consumers. The entire microgrid test system is configured, modeled and simulated using the MATLAB Simulink software, and the microgrid control system is also established to flexibly control its various operation modes. Two scenarios corresponding to two operation modes (the islanded mode and the black start mode) are examined, analyzed, and evaluated in this paper. The numerical simulation results show that the control systems of the microgrid and the BESS will maintain the microgrid in a stable operation status in both scenarios. This provides a foundation for the calculation, analysis, and reasonable selection of basic parameters for the main components in the microgrid. Additionally, it aids in effectively leveraging the integration of the solar power plant within the microgrid.

Conflict of interest

The authors declare no conflict of interest.

References

[1] J. de la Cruz, Y. Wu, J. E. Candelo-Becerra, J. C. Vásquez, and J. M. Guerrero, "Review of networked microgrid protection: architectures, challenges, solutions, and future trends," *CSEE Journal of Power and Energy Systems*, vol. 10, no. 2, pp. 448-467, 2024. http://doi.org/10.17775/CSEEJPES.2022.07980.

[2] Y. Guan, B. Wei, J. M. Guerrero, J. C. Vasquez, and Y. Gui, "An overview of the operation architectures and energy management system for multiple microgrid clusters," *iEnergy*, vol. 1, no. 3, pp. 306-314, 2022. https://doi.org/10.23919/ien.2022.0035.

[3] F. Mohammadi, B. Mohammadi-Ivatloo, G. B. Gharehpetian, M. H. Ali, W. Wei, O. Erdinç, et al., "Robust control strategies for microgrids: a review," *IEEE Systems Journal*, vol. 16, no. 2, pp. 2401-2412, 2021. https://doi.org/10.1109/jsyst.2021.3077213..

[4] V. E. Wissa, A. El Badawy, and A. El-Guindy, "Fault ride-through in grid-connected DC microgrid to improve microgrid and utility grid performance," In Proc. 2023 IEEE PES Conference on Innovative Smart Grid Technologies Middle East, Abu Dhabi, United Arab Emirates, Mar. 12-15, 2023. https://doi.org/10.1109/ISGTMiddleEast56437.2023.10078453.

[5] Z. Fan, B. Fan, and W. Liu, "Distributed control of DC microgrids for optimal coordination of conventional and renewable generators," *IEEE Transactions on Smart Grid*, vol. 12, no. 6, pp. 4607-4615, 2021. https://doi.org/10.1109/TSG.2021.3094878.

[6] S. Liu, P. Siano, and X. Wang, "Intrusion-detector-dependent frequency regulation for microgrids under denial-of-service attacks," *IEEE Systems Journal*, vol. 14, no. 2, pp. 2593-2596, 2019. https://doi.org/10.1109/jsyst.2019.2935352.

[7] J. Peng, B. Fan, and W. Liu, "Voltage-based distributed optimal control for generation cost minimization and bounded bus voltage regulation in DC microgrids," *IEEE Transactions on Smart Grid*, vol. 12, no. 1, pp. 106-116, 2020. https://doi.org/10.1109/tsg.2020.3013303.

[8] M. S. Sadabadi, "Line-independent plug-and-play voltage stabilization and $\mathscr{L}_2$ gain performance of DC microgrids," *IEEE Control Systems Letters*, vol. 5, no. 5, pp. 1609-1614, 2020. https://doi.org/10.1109/lcsys.2020.3041335.

[9] C. S. Rajan and M. Ebenezer, "Modeling operation and simulation of interconnected DC microgrids," In Proc. 2020 International Conference on Power, Instrumentation, Control and Computing, Thrissur, India, Dec. 17-19, 2020. https://doi.org/10.1109/PICC51425.2020.9362454.

[10] J. Peng, B. Fan, Q. Yang, and W. Liu, "Fully distributed discrete-time control of DC microgrids with ZIP loads," *IEEE Systems Journal*, vol. 16, no. 1, pp. 155-165, 2020. https://doi.org/10.1109/jsyst.2020.3038664.

[11] S. Sahoo, Y. Yang, and F. Blaabjerg, "Resilient synchronization strategy for AC microgrids under cyber attacks," *IEEE Transactions on Power Electronics*, vol. 36, no. 1, pp. 73-77, 2020. https://doi.org/10.1109/tpel.2020.3005208.

[12] A. S. Dahane and R. B. Sharma, "Hybrid AC-DC microgrid coordinated control strategies: a systematic review and future prospect," *Renewable Energy Focus*, vol. 49, p. 100553, 2024. https://doi.org/10.1016/j.ref.2024.100553.

[13] P. S. Kumar, "Applications of hybrid wind solar battery based microgrid for small-scale stand-alone systems and grid integration for multi-feeder systems," in *Electrical and Electronic Devices, Circuits and Materials: Technical Challenges and Solutions*, Hoboken, NJ, USA: Wiley, 2021, pp. 517-533. https://doi.org/10.1002/9781119755104.ch27.

[14] J. Qin, Y. Wan, F. Li, Y. Kang, and W. Fu, *Distributed Economic Operation in Smart Grid: Model-Based and Model-Free Perspectives*. Cham, Switzerland: Springer, 2023. https://doi.org/10.1007/978-981-19-8594-2.

[15] M. H. Saeed, W. Fangzong, B. A. Kalwar, and S. Iqbal, "A review on microgrids' challenges and perspectives," *IEEE Access*, vol. 9, pp. 166502-166517, 2021. https://doi.org/10.1109/ACCESS.2021.3135083.

[16] M. W. Altaf, M. T. Arif, S. N. Islam, and M. E. Haque, "Microgrid protection challenges and mitigation approaches—a comprehensive review," *IEEE Access*, vol. 10, pp. 38895-38922, 2022. https://doi.org/10.1109/access.2022.3165011.

[17] L. Polleux, G. Guerassimoff, J.-P. Marmorat, J. Sandoval-Moreno, and T. Schuhler, "An overview of the challenges of solar power integration in isolated industrial microgrids with reliability constraints," *Renewable and Sustainable Energy Reviews*, vol. 155, p. 111955, 2022. https://doi.org/10.1016/j.rser.2021.111955.

[18] S. Ogbikaya and M. T. Iqbal, "Dynamic simulation of a microgrid system for a university community in Nigeria," In Proc. 2022 IEEE International IOT, Electronics and Mechatronics Conference, Toronto, ON, Canada, Jun. 1-4, 2022. https://doi.org/10.1109/IEMTRONICS55184.2022.9795822.

[19] M. Simonazzi, N. Delmonte, P. Cova, and R. Menozzi, "Models for MATLAB simulation of a university campus micro-grid," *Energies*, vol. 16, no. 16, p. 5884, 2023. https://doi.org/10.3390/en16165884.

[20] R. Nandi, M. Tripathy, and C. P. Gupta, "Coordination of BESS and PV system with bidirectional power control strategy in AC microgrid," *Sustainable Energy Grids and Networks*, vol. 34, p. 101029, 2023. https://doi.org/10.1016/j.segan.2023.101029.

[21] S. I. Habibi, M. A. Sheikhi, T. Khalili, S. A. G. K. Abadi, A. Bidram, and J. M. Guerrero, "Multiagent-based nonlinear generalized minimum variance control for islanded AC microgrids," *IEEE Transactions on Power Systems*, vol. 39, no. 1, pp. 316-328, 2023. https://doi.org/10.1109/tpwrs.2023.3239793.

[22] H. N. L. Thi, T. T. Phung, H. M. V. Nguyen, N. T. H. Thi, and M. S. N. Thi, "Impact of the charging station on the quality of voltage and frequency in the microgrid," *Journal of Technical Education and Science*, vol. 19, no. SI02, pp. 77-89, 2024. https://doi.org/10.54644/jte.2024.1557.

[23] D. Q. Nguyen and M. K. Ngo, "Energy storage application for improving operation performance of distribution networks integrated with wind and solar powers," *Journal of Technical Education and Science*, vol. 19, no. 4, pp. 78-89, 2024. https://doi.org/10.54644/jte.2024.1614.

[24] K. Ni, Z. Wei, H. Yan, K.-Y. Xu, L.-J. He, and S. Cheng, "Bi-level optimal scheduling of microgrid with integrated power station based on stackelberg game," In Proc. 2019 4th International Conference on Intelligent Green Building and Smart Grid, Hubei, China, Sep. 6-9, 2019. https://doi.org/10.1109/IGBSG.2019.8886314.

[25] B. Yan, A. Kumar, and P. Zhang, "Operation optimization of microgrids with renewables," in *Microgrids: Theory and Practice*, Hoboken, NJ, USA: Wiley-IEEE Press, 2024, pp. 863-874. https://doi.org/10.1002/9781119890881.ch37.

[26] C. Yan, Y. Zou, Z. Wu, and A. Maleki, "Effect of various design configurations and operating conditions for optimization of a wind/solar/hydrogen/fuel cell hybrid microgrid system by a bio-inspired algorithm," *International Journal of Hydrogen Energy*, vol. 60, pp. 378-391, 2024. https://doi.org/10.1016/j.ijhydene.2024.02.004.

[27] J. M. Guerrero and R. Kandari, *Microgrids: Modeling, Control, and Applications*. New York, NY, USA: Academic Press, 2021. .

[28] J. Kumar, A. Agarwal, and V. Agarwal, "A review on overall control of DC microgrids," *Journal of Energy Storage*, vol. 21, pp. 113-138, 2019. https://doi.org/10.1016/j.est.2018.11.013.

[29] A. Banerjee, V. U. Pawaskar, G.-S. Seo, A. Pandey, U. R. Pailla, X. Wu, et al., "Autonomous restoration of networked microgrids using communication-free smart sensing and protection units," *IEEE Transactions on Sustainable Energy*, vol. 14, no. 2, pp. 1076-1087, 2023. https://doi.org/10.1109/TSTE.2023.3245881.